Springer Theses

Dijet Angular Distributions in Proton-Proton Collisions

At vs = 7 TeV and vs = 14 TeV

Bearbeitet von
Nele Boelaert

1. Auflage 2011. Buch. xviii, 170 S. Hardcover
ISBN 978 3 642 24596 1
Format (B x L): 15,5 x 23,5 cm
Gewicht: 450 g

Chapter 2
Introduction to QCD and Collider Physics

2.1 Quantum Chromodynamics (QCD)

Quantum chromodynamics (QCD) is the theory of the strong interaction, describing the interactions of the quarks and gluons, using the $SU(3)$ non-Abelian gauge theory of color charge [1]. The expression for the classical QCD Lagrangian density is given by:

$$\mathcal{L} = -\frac{1}{4} F^A_{\alpha\beta} F_A^{\alpha\beta} + \sum_{\text{flavors}} \bar{q}_a (i\gamma_\mu D^\mu - m)_{ab} q_b, \tag{2.1}$$

where the sum runs over the n_f different flavors of quarks ($n_f = 6$ in the SM), and α, β, γ are Lorentz indices. Throughout this entire chapter, we will work with the convention that repeated indices are implicitly summed over. $F^A_{\alpha\beta}$ is the field strength tensor derived from the gluon field $\mathcal{A}^{\mathrm{A}}_\alpha$:

$$F^A_{\alpha\beta} = [\partial_\alpha \mathcal{A}^A_\beta - \partial_\beta \mathcal{A}^A_\alpha - g_s f^{ABC} \mathcal{A}^B_\alpha \mathcal{A}^C_\beta] \tag{2.2}$$

The capital indices A, B and C run over the eight degrees of freedom of the gluon field. Note that it is the third (non-Abelian) term in the above expression that makes the gluons have self-interactions. This means that, unlike the photon in QED, the carrier of the color force is itself colored, a property that is giving rise to asymptotic freedom (see further in the text). The numbers f^{ABC} are structure constants of the $SU(3)$ group. Quark fields q_a ($a = 1, 2, 3$) are in triplet color representation, with colors red (r), green (g) and blue (b).

The strong coupling strength g_s in Eq. 2.2 is used to define the strong coupling constant $\alpha_s = g_s^2/4\pi$. D in Eq. 2.1 stands for the covariant derivative, which takes, acting on triplet and octet fields respectively, the form:

$$(D_\alpha)_{ab} = \partial_\alpha \delta_{ab} + ig(t^C \mathcal{A}^C_\alpha)_{ab} \tag{2.3}$$

N. Boelaert, *Dijet Angular Distributions in Proton–Proton Collisions*, Springer Theses,
DOI: 10.1007/978-3-642-24597-8_2, © Springer-Verlag Berlin Heidelberg 2012

$$(D_\alpha)_{AB} = \partial_\alpha \delta_{\mathrm{AB}} + ig(T^C \mathcal{A}_\alpha^C)_{AB}, \tag{2.4}$$

where t and T are matrices in the fundamental and adjoint representations of $SU(3)$ respectively.

2.1.1 Perturbative QCD (pQCD)

By adding a gauge-fixing term to the classical QCD Lagrangian (Eq. 2.1):

$$\mathcal{L}_{\mathrm{gauge-fixing}} = -\frac{1}{2\lambda}(\partial^\alpha \mathcal{A}_\alpha^A)^2, \tag{2.5}$$

and a so-called ghost Lagrangian which is derived from a complex scalar field η^A and is needed because the theory is non-Abelian:

$$\mathcal{L}_{\mathrm{ghost}} = \partial_\alpha \eta^{A\dagger}(D^\alpha_{AB}\eta^B), \tag{2.6}$$

any process can be calculated in a perturbative way using Feynman rules which are obtained from replacing covariant derivatives by appropriate momenta. The Feynman rules in a covariant gauge are given in Fig. 2.1. However, a perturbative calculation generally requires 4-dimensional integrations over intermediate momentum states arising from gluon quantum fluctuations, which suffer from ultraviolet divergences.

A *renormalization* procedure is needed to remove these divergences, which essentially means that the Lagrangian is rewritten so that bare masses and coupling strengths are eliminated in favor of their physically measurable counterparts, giving rise to a renormalized Lagrangian [2]. Modified Feynman rules are derived from this Lagrangian and singularities in the contributions from individual diagrams are now absorbed by the physical quantities, leading to a finite result at the end.

Several renormalization methods are possible, and the exact definitions of physical quantities—masses and coupling constants—depend on the specific renormalization scheme used in the theory, but common to all schemes is the inclusion in the renormalized Lagrangian of a new, arbitrary parameter, with the dimension of mass, needed to define the physical quantities.This parameter is often called the renormalization scale μ_R. It appears in the intermediate parts of a calculation, but cannot ultimately influence the relations between physical observables.

A consequence of renormalization is that the definition of the physically observable quantities not only depends on μ_R, but also becomes scale dependent; when the theory is normalized at a scale μ_R but then applied to a very different scale Q (of the order of the momentum invariants of the reaction), the coupling constants and masses adjust to that scale, a process which is commonly referred to as the *running* of the coupling constants and masses.

The running of the coupling constant α_s is controlled by the β function [3], which is derived from the statement that a physical observable cannot depend on μ_R:

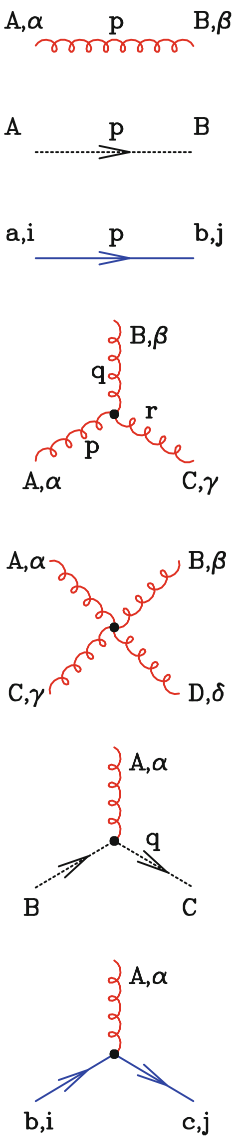

$$\delta^{AB}\ \left[-g^{\alpha\beta}+(1-\lambda)\frac{p^\alpha p^\beta}{p^2+i\epsilon}\right]\frac{i}{p^2+i\epsilon}$$

$$\delta^{AB}\ \frac{i}{(p^2+i\epsilon)}$$

$$\delta^{ab}\ \frac{i}{(\not{p}-m+i\epsilon)_{ji}}$$

$$-g\ f^{ABC}[(p-q)^\gamma g^{\alpha\beta}+(q-r)^\alpha g^{\beta\gamma}+(r-p)^\beta g^{\gamma\alpha}]$$

(all momenta incoming)

$$\begin{aligned}&-ig^2\ f^{XAC}f^{XBD}\ [g^{\alpha\beta}g^{\gamma\delta}-g^{\alpha\delta}g^{\beta\gamma}]\\&-ig^2\ f^{XAD}f^{XBC}\ [g^{\alpha\beta}g^{\gamma\delta}-g^{\alpha\gamma}g^{\beta\delta}]\\&-ig^2\ f^{XAB}f^{XCD}\ [g^{\alpha\gamma}g^{\beta\delta}-g^{\alpha\delta}g^{\beta\gamma}]\end{aligned}$$

$$g\ f^{ABC}q^\alpha$$

$$-ig\ (t^A)_{cb}\ (\gamma^\alpha)_{ji}$$

Fig. 2.1 Feynman rules for QCD in a covariant gauge from gluons (*curvy red lines*), fermions (*solid blue lines*) and ghosts (*dotted black lines*) [1]

$$Q\frac{\partial\alpha_s}{\partial Q}\equiv 2\beta_{\text{QCD}}=-\frac{\beta_0}{2\pi}\alpha_s^2-\frac{\beta_1}{4\pi^2}\alpha_s^3-\mathcal{O}(\alpha_s^4), \tag{2.7}$$

with

$$\beta_0=11-\frac{2}{3}n_f \tag{2.8}$$

$$\beta_1 = 51 - \frac{19}{3} n_f \tag{2.9}$$

Given that α_s is known (from experiment) at a certain scale Q_0, Eq. 2.7 can be used to calculate its value at any other scale Q:

$$\log(Q^2/Q_0^2) = \int_{\alpha_s(Q_0)}^{\alpha_s(Q)} \frac{\mathrm{d}\alpha}{\beta(\alpha)} \tag{2.10}$$

Equation 2.10 is solvable using the leading-order (LO) term of $\beta(\alpha)$ only, which gives:

$$\alpha_s(Q) = \frac{\alpha_s(Q_0)}{1 + \frac{\beta_0}{2\pi}\alpha_s(Q_0)\ln(Q^2/Q_0^2)} \approx \alpha_s(Q_0)\Big(1 - \frac{\beta_0}{2\pi}\alpha_s(Q_0)\ln(Q^2/Q_0^2)\Big) \tag{2.11}$$

Another way to solve Eq. 2.7 is by introducing a dimensional parameter Λ, representing the mass scale at which α_s becomes infinite. This way, we get:

$$\alpha_s(Q) = \frac{4\pi}{\beta_0 \ln(Q^2/\Lambda^2)}\left[1 - \frac{2\beta_1}{\beta_0^2}\frac{\ln[\ln(Q^2/\Lambda^2)]}{\ln(Q^2/\Lambda^2)} + \mathcal{O}(\ln^{-2}(Q^2/\Lambda^2))\right] \tag{2.12}$$

Note that in Eqs. 2.11 and 2.12 the running of α_s with Q is logarithmic, so that we do not need to worry too much about choosing Q precisely.

Equation 2.12 illustrates the hallmark of QCD, namely *asymptotic freedom*: $\alpha_s \to 0$ as $Q \to \infty$. It also shows that QCD becomes strongly coupled at $Q \sim \Lambda$, which is at about 200 MeV. This implies that perturbative methods can be used in the short-distance limit, at scales Q much larger than Λ. The fact that the strong force becomes strong at larger distances, means that color charged particles cannot be isolated singularly and cannot be observed as states that propagate over macroscopic distances, a property which is called *confinement*. Only color singlet states composed of quarks and gluons, i.e. hadrons, can be observed. We will talk about hadronization in Sect. 2.5. Perturbative methods are no longer a valid approximation in this area.

Experiments usually report the strong coupling at the scale corresponding to the Z mass ($M_Z = 91.2$ GeV). The world average of $\alpha_s(M_Z)$ is determined from measurements which are based on QCD calculations in complete next-to-next-to leading order (NNLO) perturbation theory, giving $\alpha_s(M_Z) = 0.1182 \pm 0.0027$ [4].

2.2 The Parton Model

The high-energy interactions of hadrons are described by the QCD parton model [5, 6]. The basic idea of this model is that the hard scattering between two hadrons can be understood as the interaction between the partons—quarks and gluons with their masses neglected—that make up the hadrons.

A hadron consists of a number of valence quarks (e.g. *uud* for the proton) and an infinite sea of gluons and light quark-antiquark ($q\bar{q}$) pairs. The valence quarks carry the hadron's electric charge and baryon quantum numbers. When probed at a scale Q, the sea contains all quark flavors with mass $m_q \ll Q$. The gluons carry about 50% of the proton's total momentum. A *parton distribution function* (PDF) is used to denote the probability distribution that a quark, antiquark or gluon carries a given fraction of the momentum of the hadron.

The sea is not static, there is a continuous movement of gluons splitting and recombining into $q\bar{q}$ pairs, and both quarks and gluons can emit and absorb gluons as well. These processes imply that the transverse momenta of partons inside the hadron are not restricted to small values, and that the PDFs describing the partons depend on the scale Q that the hadron is probed with, a behavior which is known as a violation of Bjorken Scaling. At leading order, the dependence on Q is logarithmic.

If $q(x, Q)$ is the PDF describing quark Q, then $q(x, Q)\mathrm{d}x$ represents the probability that Q carries a momentum fraction between x and $x + \mathrm{d}x$ when the hadron is probed at a scale Q.

Each hadron has its own set of PDFs and separate PDFs are used for describing the sea and the valence quarks; the PDFs for the valence quarks are flavor specific, but QCD guarantees flavor number conservation of the sea quarks.

For example, for the proton at a scale of about 1 GeV, we can write:

$$u(x, Q) = u_v(x, Q) + u_s(x, Q) \tag{2.13}$$

$$d(x, Q) = d_v(x, Q) + d_s(x, Q) \tag{2.14}$$

Taking into account quark number conservation, the following sum rules apply:

$$\int_0^1 \mathrm{d}x\, u_v(x, Q) = 2 \tag{2.15}$$

$$\int_0^1 \mathrm{d}x\, d_v(x, Q) = 1 \tag{2.16}$$

And experimentally, it was found that:

$$\sum_q \int_0^1 \mathrm{d}x\, x[q(x, Q) + \bar{q}(x, Q)] \approx 0.5, \tag{2.17}$$

meaning that the quarks carry only about half of the proton's momentum (and the gluons the other half).

When a quark emits a gluon, it can acquire a large momentum k_T with probability proportional to $\alpha_s \mathrm{d}k_T^2/k_T^2$ at large k_T. This splitting diverges in the collinear region $(k_T \to 0)$. This is not a physical divergence; it simply means that perturbative QCD is not a valid approximation in this region.

The way to solve this is to renormalize the PDFs by introducing a *factorization scale* μ_f. Similar to the renormalization scale, the factorization scale absorbs the divergences coming from interactions that are not calculable in perturbation theory. This way, the PDFs become scale dependent, just like the strong coupling constant discussed in the previous section.

Perturbative QCD carries no absolute prediction of the PDF, but does predict how the PDF scales with Q; these are the so called DGLAP (Dokshitzer–Gribov–Lipatov–Altarelli–Parisi) evolution equations [7–9]:

$$t\frac{\partial}{\partial t}\begin{pmatrix} q_i(x,t) \\ g(x,t) \end{pmatrix} = \frac{\alpha_s(t)}{2\pi}\sum_{q_i,\bar{q}_j}\int_x^1 \frac{\mathrm{d}\,z}{z}\begin{pmatrix} P_{q_j\to q_i g}(z,\alpha_s(t)) & P_{g\to q_i\bar{q}_i}(z,\alpha_s(t)) \\ P_{q_j\to g q_i}(z,\alpha_s(t)) & P_{g\to gg}(z,\alpha_s(t)) \end{pmatrix} \begin{pmatrix} q_j(x/z,t) \\ g(x/z,t) \end{pmatrix} \tag{2.18}$$

Here, $t = -Q^2$, $q_{i,j}(x,t)$ and $g(x,t)$ are the quark and gluon parton distribution functions respectively, and the functions $P_{a\to bc}(z)$ are the so called unregularized splitting kernels [1]. We will derive the DGLAP equations in Sect. 2.4

The DGLAP evolution equations specify the evolution of the parton density functions in the same way as the β function (Eq. 2.7) specifies the evolution of the strong coupling constant. When solving Eq. 2.18 to the leading order, the term $\partial t/t$ will cause the PDFs to obey a logarithmic dependence on $t = -Q^2$.

The DGLAP equations do allow for the evolution of the PDFs from a certain reference scale Q_0 onwards, but data are still needed to determine its value at the scale Q_0. Deep inelastic lepton-hadron scattering measurements are an excellent tool for probing PDFs and the reference scale is typically chosen around 1 GeV. Note that PDFs are universal, i.e. they can be determined from one type of experiment (e.g. $e^- p$ collisions) and used in another (e.g. pp collisions). In the past, leading-order matrix elements together with lowest order running of α_s (see Eq. 2.11) were used for the fit. Nowadays, also next-to-leading order (NLO) and even NNLO PDFs—resulting from a fit to NLO or NNLO matrix elements and a higher order running of α_s—have become available.

Historically there are two major collaborations working on PDFs: the CTEQ [10], and the MRST [11], nowadays MSTW [12], collaboration. Figure 2.2 shows the MRST2004NLO PDFs multiplied with x, for the up and down quark and the gluon inside the proton at $Q^2 = 10^4\,\mathrm{GeV}^2$. The gluon distribution is scaled with a factor 1/10 in order to fit into the plot. Note that the gluon distribution dominates at small values of x.

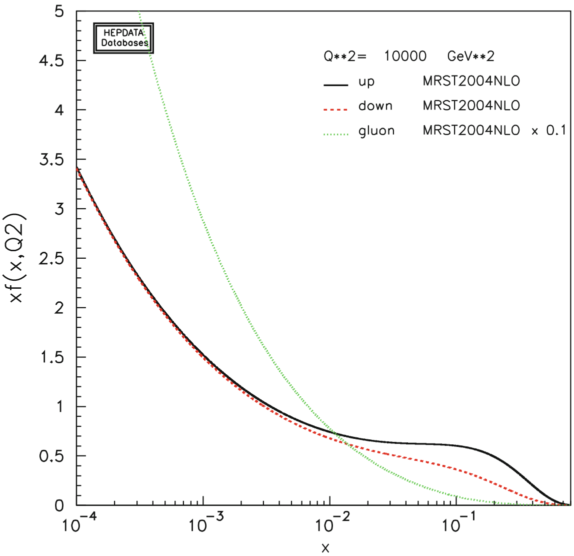

Fig. 2.2 Proton parton distribution functions multiplied with x. The gluon distribution is scaled with a factor 1/10 [11]

2.3 Hard Scattering Processes in Hadron Collisions

When two hadrons collide at high energy, most of the collisions involve only soft interactions of the constituent quarks and gluons. Such interactions cannot be treated using perturbative QCD, because α_s is large when the momentum transfer is small. In some collisions however, two quarks or gluons will exchange a large momentum. In those cases, the elementary interaction takes place very rapidly compared to the internal time scale of the hadron wavefunctions, so the lowest order(s) QCD prediction should accurately describe the process.

The cross section for such a process can be written as a factorized product of short and long distance processes:

$$\sigma(P_1, P_2) = \sum_{i,j} \int \mathrm{d}x_1 \mathrm{d}x_2 f_i(x_1, \mu_F^2) f_j(x_2, \mu_F^2) \hat{\sigma}_{i,j}(\mu_R^2, \mu_F^2), \tag{2.19}$$

where P_1 and P_2 denote the momenta of the incoming hadrons. Figure 2.3 shows this schematically. The momenta of the partons that participate in the hard interaction are $p_1 = x_1 P_1$ and $p_2 = x_2 P_2$. The functions $f_i(x_1, \mu_F^2)$ and $f_j(x_2, \mu_F^2)$ are the usual QCD quark or gluon PDFs, defined at a factorization scale μ_F, which take into account the long-distance effects. It is in this sense that μ_F can be thought of as the scale which separates long- and short-distance physics.

The short-distance cross section for the scattering of partons of types i and j is denoted by $\hat{\sigma}_{i,j}$. Since the coupling is small at high energy, $\hat{\sigma}_{i,j}$ can be calculated as a perturbation series in α_s.

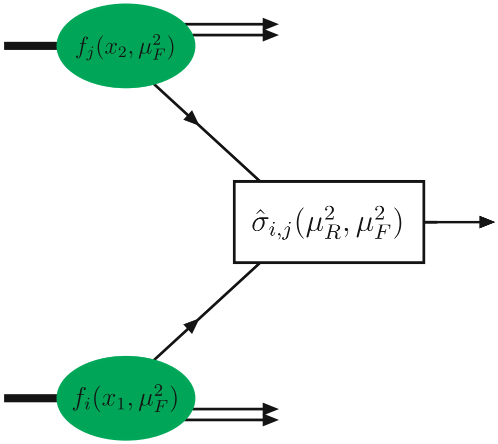

Fig. 2.3 The parton model description of a hard scattering process

At leading order, $\hat{\sigma}_{i,j}$ is identical to the normal parton scattering cross section and the dependence on μ_F disappears, but at higher order, long-distance parts in the parton cross section need to be removed and factored into the parton distribution functions.

Note that if calculated to all orders, the cross section should be independent of the factorization and renormalization scales:

$$\frac{\partial \sigma}{\partial \mu_F} = \frac{\partial \sigma}{\partial \mu_R} = 0 \tag{2.20}$$

In practice, one is restricted to calculations at low orders, for which the residual dependence on μ_F and μ_R can be appreciable.

Equation 2.19 is a prediction of the cross section with partons in the outgoing state. Experiments however, measure hadrons and not partons due to confinement. The non-perturbative process that transforms partons into hadrons is called hadronization and this will be discussed in Sect. 2.5. But first we will discuss parton showers in the next section.

2.4 Parton Branching

As discussed in Sect. 2.3, the hard collision between two hadrons, can be understood as the collision between two partons. The first terms in the perturbative QCD expansion, usually suffice to describe successfully the hard interaction between these two partons, because the scale of this process is large.

However, in some regions of the phase space, higher order terms are enhanced and cannot be neglected. For example, we have seen in Sect. 2.2 about the parton model that when a quark emits a gluon, perturbation theory fails to describe the process in the collinear region.

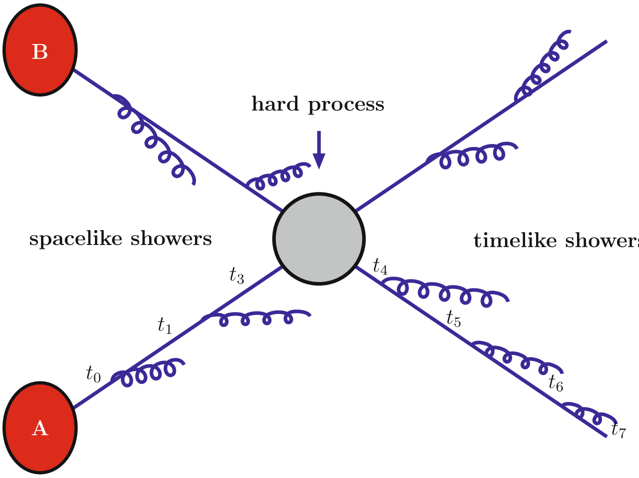

Fig. 2.4 Schematic illustration of the hard scattering process and the softer showers. For initial state branchings, t is increasing towards the hard scattering by means of successive small-angle emissions ($t_0 < t_1 < t_3$). The opposite is true for final state branching, where t is decreasing after every branching ($t_4 > t_5 > t_6 > t_7$)

Enhanced higher-order terms occur in processes where a soft gluon is emitted or when a gluon or light quark splits into two almost collinear partons. *Parton branching* is the common name for these soft and collinear configurations.

In collision processes, parton branching typically happens for the ingoing and outgoing quarks and gluons of the hard interaction. The incoming quark, initially with low virtual mass-squared and carrying a fraction x of the hadron's momentum, moves to more virtual masses and lower momentum fractions by successive small-angle emissions, and finally undergoes the hard scattering which happens at a scale Q. After the collision, the outgoing parton of the hard scattering process has initially a large positive mass-squared, which then gradually decreases by consecutive parton emissions.

Figure 2.4 shows schematically a hard hadron collision. Two hadrons (A and B) are coming in and one incoming parton in each hadron gets selected, and undergoes a hard scattering, resulting in outgoing partons. The hard scattering of the incoming partons which happens at a scale Q, can be calculated using perturbative QCD. But all incoming and outgoing partons undergo branchings as well, giving rise to the so called parton showers (and to scale dependent PDFs). A lower order perturbative calculation fails to describe the shower behavior, but perturbative QCD calculations become too complicated at higher orders to be of practical use. We will show that an approximate perturbative treatment of QCD to all orders is adequate at describing the branching physics.

A distinction needs to be made between partons that are incoming lines in the Feynman diagram describing the hard interaction, and partons that are outgoing lines. An incoming parton has a negative (virtual) mass-squared. Therefore its branching process is called spacelike, giving rise to initial state showers. The opposite is true for outgoing branching partons. These partons have a positive mass-squared and their branching is said to be timelike. They give rise to final state showers.

A branching can be seen as a $a \to bc$ process, where A is called the mother and b and c the daughters. Each daughter is free to branch as well, so that a shower-like structure can evolve.

For a timelike branching, we assume that the mass of the mother is much higher than the masses of the daughters. For a spacelike branching, we assume that the daughter that will finally take part in the hard interaction has a much larger virtuality than the other partons.

In the approximation of small angle scattering, the branching kinematics can be described by two variables, z and t. We define z as the fraction of energy carried by daughter b: $z = E_b/E_a = 1 - E_c/E_a$. The variable t can have different interpretations, but always has the dimensions of squared mass. Here we will define t as the mass squared of the mother ($t \equiv p_a^2$) for timelike branching and as the absolute value of the mass squared of the daughter ($t \equiv |p_b^2|$) for spacelike branching.

In terms of z and t, the differential probability that one branching occurs is given by:

$$\mathrm{d}\mathcal{P}_a = \sum_{b,c} \frac{\alpha_s}{2\pi} P_{a\to bc}(z) \frac{\mathrm{d}t}{t} \mathrm{d}z, \tag{2.21}$$

where the sum runs over all branchings the parton is allowed to make. The functions $P_{a\to bc}(z)$ are the so called splitting kernels. They are written as a perturbation series and, at lowest order, can be interpreted as the probability of finding a parton of type b in a parton of type a with a momentum fraction z. For example, for the splitting of a gluon into a quark antiquark pair, we have at lowest order that $P_{g\to q\bar{q}}(z) \propto (z^2 + (1-z)^2)$. We integrate Eq. 2.21 over z in order to get the branching probability for a certain t value:

$$\mathcal{I}_{a\to bc}(t) = \int_{z^-(t)}^{z^+(t)} \mathrm{d}z \frac{\alpha_s}{2\pi} P_{a\to bc}(z), \tag{2.22}$$

where we have considered one type of branching only. In principle z can vary between 0 and 1, but because most splitting kernels suffer from infrared singularities at $z = \{0, 1\}$, we need to introduce an explicit cut-off. Physically, this can be understood by saying that branchings close to the integration limits are unresolvable; they involve the emission of an undetectably soft parton. Alternatively, the plus prescription of the splitting function can be used instead of $z^-(t)$ and $z^+(t)$ [7–9].

The naïve probability that a branching occurs in the range $[t, t + \mathrm{d}t]$, is given by $\sum_{b,c} \mathcal{I}_{a\to bc}(t)\mathrm{d}t/t$, and thus the probability of no emission is $1-\sum_{b,c} \mathcal{I}_{a\to bc}(t)\mathrm{d}t/t$.

This is however, not correct when we consider multiple branchings. Note that from Heisenberg's principle, t fills the function of a kind of inverse time squared for the shower evolution; t is constrained to be gradually decreasing away from the hard scattering in final state showers, and to be gradually increasing towards the hard scattering in initial state showers.

This means that the probability for branching at a time t needs to take into account the probability that the parton has not branched at earlier times $t_0 < t$. The probability that a branching did not occur between t_0 and t, is given by the Sudakov form factor [13]:

$$\mathcal{P}_{\text{no-branching}}(t_0, t) = \exp\left\{ -\int_{t_0}^{t} \frac{\mathrm{d}t'}{t'} \sum_{b,c} \mathcal{I}_{a\to bc}(t') \right\} = S_a(t), \tag{2.23}$$

giving rise to the actual probability that a branching occurs at time t:

$$\begin{aligned} \frac{\mathrm{d}\mathcal{P}_a}{\mathrm{d}t} &= -\frac{\mathrm{d}\mathcal{P}_{\text{no-branching}}(t_0, t)}{\mathrm{d}t} = \left(\frac{1}{t}\sum_{b,c}\mathcal{I}_{a\to bc}(t)\right) S_a(t) \\ &= \left(\frac{1}{t}\sum_{b,c}\int_{z^-(t)}^{z^+(t)} \mathrm{d}z \frac{\alpha_s}{2\pi} P_{a\to bc}\right) \exp\left\{ -\int_{t_0}^{t} \frac{dt'}{t'} \sum_{b,\,c} \int_{z^-(t')}^{z^+(t')} \mathrm{d}z \frac{\alpha_s}{2\pi} P_{a\to bc} \right\} \end{aligned} \tag{2.24}$$

The first term in the right hand side of the above equation is the naïve branching probability. The other term is needed to deal with the fact that partons that have already branched can no longer branch. This is similar to the radioactive decay.

Equation 2.24 can be used to simulate jet production, and therefore forms the basis for parton showers implemented in many Monte Carlo event generators [14].

Because inside the hadron, sea quarks and gluons undergo the same branchings as described in this section, the evolution of PDFs can be described with the same techniques [1]. These are the DGLAP equations, which were shown in Sect. 2.2 (see Eq. 2.18).

The DGLAP equations are not applicable in all regions of phase space. As a matter of fact, it turns out that when $\ln(t/\Lambda^2) \ll \ln(1/x)$, i.e. for small values of x, not all leading terms are included; important contributions in terms of $\ln(1/x)$ are neglected. The resummation of terms proportional to $\alpha_s \ln(1/x)$ to all orders, retaining the full t dependence and not just the leading $\ln(t)$ is accomplished by the Balitsky–Fadin–Kuraev–Lipatov (BFKL) [15, 16] equation.

2.5 Hadronization

Due to color confinement, quarks and gluons cannot propagate freely over macroscopic distances. When two quarks are close together, the strong force between them is relatively weak (asymptotic freedom), but when they move farther apart, the force becomes much stronger (confinement). The potential between the quarks increases linearly with their mutual separation, and at some distance, it becomes much easier to create a new quark-antiquark pair than to keep pulling against the ever-increasing potential. This process is repetitive and the newly created quarks and antiquarks will combine themselves into hadrons.

In a collision experiment, all outgoing partons will therefore undergo parton showering and transform themselves into hadrons, forming jets, i.e. sprays of hadrons, which are then experimentally detected. The process is called *hadronization*.

Hadronization cannot be calculated in perturbative QCD, because it happens in a region where α_s is too strong. But still, jets are very useful for our understanding of QCD. The reason is that by the uncertainty principle, a hard interaction at a typically large scale Q occurs at a distance scale of the order of $1/Q$, while the subsequent hadronization processes occur at a much later time scale characterized by $1/\Lambda$, where Λ is the scale at which the strong coupling becomes strong. The interactions that change quarks and gluons into hadrons, certainly modify the outgoing state, but they occur too late to modify the original probability for the event to happen, which can therefore be calculated in perturbation theory. Each hadron appears in the final state roughly in the same direction as the quark or gluon it originated from. The cross section for a single hadron is therefore closely related to the underlying partonic direction, and for a good jet finding algorithm, the extension to jet cross sections can be made. We will talk about jets in detail in later chapters.

Popular models describing hadronization are the Lund string model [17] and the cluster model [18]. In all models, color singlet structures are formed out of color connected partons, and are decayed into hadrons preserving energy and momentum.

2.6 Monte Carlo Event Generators

As already mentioned in the introductory chapter, particle collision experiments are of high importance for testing theories. In order to be able to interpret scattering experiments in terms of an underlying theory, a comparison between events simulated according to that specific theory and data is needed. Since nature is fundamentally probabilistic, the generated events need to exhibit the same statistical fluctuations. Pseudo-randomness can be computed using suited Monte Carlo techniques.

The generation of an event is done using a factorized approach, and the major steps are:

1. the hard scattering process
2. initial and final state radiation (i.e. parton showers)
3. hadronization and beam remnants
4. multiple interactions

The first three steps were discussed in this chapter, but more generator-specific information can be found in Ref. [14].

Besides a hard scattering, additional interactions between partons occur in the event, which are called multiple interactions and cannot be neglected.

A beam remnant is what remains of the incoming beam after one of its partons has initiated the hard scattering. Because the beam remnants are no longer color neutral, they need to be included into the calculation.

Due to its high complexity, the hard scattering is usually calculated at leading order. Programs with higher order scatterings exist, but these programs do not include the other steps of the event generation (i.e. they are not *complete*).

The work in this thesis is done using four generators:

- PYTHIA [14, 19]
- NLOJET++ [20]
- JETRAD [21]
- GravADD [22]

PYTHIA is a complete, multi-purpose event generator with leading-order matrix elements. Within many experimental collaborations, this program has become the standard for providing event properties in a wide range of reactions, within and beyond the Standard Model, with emphasis on those that include strong interactions, directly or indirectly, and therefore multihadronic final states. While the first releases were coded in Fortran [14], more current releases have been written in C++ [19] .

NLOJET++ and JETRAD use a next-to-leading order (NLO) description of the hard scattering, but parton showers, hadronization, beam remnants and multiple interactions are not implemented. NLO Monte Carlo techniques will be the topic of Chap. 3 .

GravADD is a complete generator for black holes and gravitational scattering in large extra dimensions, in addition to standard QCD processes. See Chap. 5 for a detailed description.

References

1. R.W. Ellis, W.J. Stirling, B.R. Webber, *QCD and Collider Physics*. Cambridge Monographs on Particle Physics Nuclear Physics and Cosmology (Cambridge University Press, Cambridge, 1996)
2. M.E. Peskin, D.V. Schroeder, *An Introduction to Quantum Field Theory* (Westview Boulder, CO, 1995)
3. C. Amsler et al., Review of particle physics. Phys. Lett. **B667**, 1 (2008)
4. S. Bethke, α_s at Zinnowitz 2004. Nuclear Physics B- Proceedings Supplements, **135** 345–352 hep-ex/0407021 (2004)
5. J.D. Bjorken, Asymptotic sum rules at infinite momentum. Phys. Rev. **179**, 1547–1553 (1969)
6. R.P. Feynman, *Photon-Hadron Interactions* (WA Benjamin Reading Mass, New York, 1972)
7. G. Altarelli, G. Parisi, Asymptotic freedom in parton language. Nucl. Phys. **B126**, 298 (1977)
8. Y.L. Dokshitzer, Sov. Phys. JETP **46**, 641 (1977)
9. V.N. Gribov, L.N. Lipatov, Yad. Fiz. **15**, 781 (1972)
10. P.M. Nadolsky, H.L. Lai, Q.-H. Cao, J. Huston, J. Pumplin, D. Stump, W.K. Tung, C.P. Yuan, Implications of CTEQ global analysis for collider observables. Phys. Rev. **D78**, 013004 (2008)
11. A.D. Martin, R.G. Roberts, W.J. Stirling, R.S. Thorne, Physical gluons and high-ET jets. Phys. Lett. **B604**, 61–68 (2004) (hepph0410230)

12. A.D. Martin, W.J. Stirling, R.S. Thorne, G. Watt, Parton distributions for the LHC. EPJ C **63**, 189–285 (2009)
13. V.V. Sudakov, Vertex parts at very high-energies in quantum electrodynamics. Sov. Phys. JETP **3**, 65–71 (1956)
14. T. Sjöstrand, S. Mrenna, P. Skands, PYTHIA 6.4 physics and manual. JHEP **0605**, 026 (2006) (hep-ph0603175)
15. E.A. Kuraev, L.N. Lipatov, V.S. Fadin, The pomeranchuk singularity in nonabelian gauge theories. Sov. Phys. JETP **45**, 199–204 (1977)
16. Y.Y. Balitsky, L.N. Lipatov, The pomeranchuk singularity in quantum chromodynamics. Sov. J. Nucl. Phys. **28**, 822–829 (1978)
17. B. Andersson, G. Gustafson, G. Ingelman, T. Sjostrand, Parton fragmentation and string dynamics. Phys. Rept. **97**, 31–145 (1983)
18. R.D. Field, S. Wolfram, A QCD model for e^+e^- annihilation. Nucl. Phys. B **213**, 65–84 (1983)
19. T. Sjöstrand, S. Mrenna, P. Skands, A brief introduction to PYTHIA 8.1. JHEP **05**, 026 (2007) (hep-ph07103820)
20. Z. Nagy, Next-to-leading order calculation of three-jet observables in hadron–hadron collision. Phys. Rev. **D68**, 094002 (2003) (hep-ph0307268)
21. W.T. Giele, E.W.N. Glover, D.A. Kosower, Higher order corrections to jet cross sections in hadron colliders. Nucl. Phys. B **B403**, 633 (1993) (hep-ph9302225)
22. L. Lönnblad, M. Sjödahl, Classical and non-classical ADD-phenomenology with high-ET jet observables at collider experiments. JHEP **0610**, 088 (2006) (hep-ph/0608210)